Biophysics

AIMS Biophysics, 8(1): 80–102.
DOI: 10.3934/biophy.2021006
Received: 05 November 2020
Accepted: 20 December 2020
Published: 05 January 2021

http://www.aimspress.com/journal/biophysics

Research article

On slip of a viscous fluid through proximal renal tubule with linear reabsorption

Abdul M. Siddiqui[1], **Getinet A. Gawo**[1] **and Khadija Maqbool**[2,*]

[1] Pennsylvania State University, 1031 Edgecomb Ave, York, PA 17403, USA
[2] Department of Mathematics and Statistics, International Islamic University, Islamabad 44000, Pakistan

* **Correspondence:** Email: khadija.maqbool@iiu.edu.pk; Tel: +92519019393.

Abstract: The hydrodynamical problem of flow in proximal renal tubule is investigated. Axisymmetric flow of viscous, incompressible fluid through the proximal renal tubule that undergoes linear reabsorption with slip at the wall is considered. The stream function is used to transform the governing equations to system of ordinary differential equations. The analytical solutions for velocity components, pressure distribution, fractional reabsorption and the shear stress are found. The effect of slip parameter and reabsorption rate on the flow have been investigated. The points of extreme values for the axial and radial velocity components are identified. The solution is applied to physiological data from human and rat kidney, and the results are presented in tables and graphs.

Keywords: proximal tubule; linear reabsorption; slip boundary; fractional reabsorption; flow rate

1. Introduction

The importance of kidneys in controlling body water and salt content through filtration process has triggered interest among renal physiologists and mathematicians to better understand the hydrodynamics in the smaller parts of a kidney. The functional component of a kidney is called nephron or renal tubule, and each human kidney contains one million nephrons. This functional unit plays the vital role in the process of filtration and regulation. The two kidneys receive over a liter of blood every minute and eliminate nearly 1.5 liter of excess water and waste product in the form of urine every day, if the kidneys function is not normal that would cause health problem. Once the blood is supplied to the kidney, the filtration process passes through two different steps in the nephron: glomerulus and renal tubule. In the first step, glomerulus creates an ultra-filtrate of body by sieving out blood cells and large plasma proteins and in the second step, part of the filtrate reabsorbed back to our body in the renal tubule, otherwise the body would lose valuable materials and water. As described in [1], 80% of the original filtrate is reabsorbed back to the system at the end of the tubule.

The study of viscous flow in a permeable tube has wide application in medical and biological problems. Different mechanisms such as, membrane filtration, blood flow through arteries and veins, urine flow through proximal tubule of a kidney and process of artificial dialysis depend upon the modelling of permeable narrow tubes. Different researchers [2,3,4,5] proposed experimental and theoretical models of narrow permeable conduit. In the last couple of decades extensive research have been done on the study of hydrodynamics flow through a renal tubule. Macey [1], [6] was the pioneer who did research in this area. Macey in [1] found the solution to the radial and axial velocity component and mean pressure drop for axially symmetric flow in a tube with linear wall reabsorption. Macey [6] also studied the physiological quantities when the wall reabsorption is exponential function of the axial length. Gilmer [7] with his coauthors has discussed the resistance property of the fluid through the renal tubule of rat. Achala and Shreenivas in [8] found the estimate for extreme values of the axial velocity components. The hydrodynamics of viscous fluid flow through a porous slit with linear absorption was studied by Haroon et.al [9]. In this work the authors converted the system of partial differential equations (PDEs) to a single ordinary differential equation (ODE) with the help of stream function, and they found the explicit expression for velocity components, pressure, and wall shear stress in rectangular coordinate geometry.

The behavior of fluid flow can be observed by the viscosity or shear stress that are related by the stress strain relationship. The viscosity and shear stress can be measured in viscous flow if fluid adheres no-slip condition on the wall. Many fluids like polymers and solutions do not satisfy the no-slip boundary condition on the wall, these fluids slip with different slip velocity at wall depending upon the magnitude of shear stress. First time Navier [10] presented the slip boundary condition and Helmholtz [11] improved the slip boundary condition by introducing the slip coefficient occurring due to slip on the wall. Mooney [12] further improved the assumption of Navier, and he concluded that slip velocity depends more generally on the shear stress at the wall and validated his research on experimental technique. Different researchers [13,14,15,16,17] used the power law equation to relate the slip velocity and shear stress at the wall. In this study we have focused on the slip velocity which is linearly proportional to the shear stress on the wall. Rao et al. [18] study the slip effect of fluids in a channel, later Elshahed [19] extended his research for blood flow with slip boundary condition. Few studies [20,21,22] have been seen in literature for the different flow geometries with slip boundary conditions. As indicated in the work of Priezjev et al. [23], the value of effective slip-length affects hydrodynamic quantities. For highly lubricated tube the non-vanishing axial profile is expected. Palatt et al. [24] studied the velocity and pressure of the flow. Extending this work, A. M. Siddiqui et al. [25] added the slip effect to the problems and found expressions for velocity components, pressure drop, shear stress and fractional reabsorption.

The purpose of this paper is to study the effect of slip condition on a flow through proximal tubule that undergoes linear reabsorption. For this study, we have considered an incompressible viscous filtrate that passes through a proximal tubule. This work is important to understand physiological quantities of a filtrate flow through proximal tubule when slip is observed near the wall.

To the best knowledge of the authors, no work has been reported so far that combines slip condition and linear reabsorption to a flow through proximal tubule.

This paper is organized in five sections. Section 2 formulates the problem and underlying assumptions considered in this study. In section 3 the coupled PDEs are converted into a single ODE and analytical solutions to axial velocity, radial velocity, and average pressure drop and wall shear stress are discussed. Sections 4 discusses application of the result by taking physiological data of human kidney for linear and uniform reabsorption with slip and no slip boundary condition. Numerical results are presented through graphs. Finally, in section 5 conclusion of the present research is made through the main observations.

2. Problem formulation

Consider an incompressible viscous proximal fluid that passes through a permeable proximal tubule of radius R and length L. Cylindrical coordinates are used to describe the dynamics, because the fluid has velocities both in the radial and axial direction, which is described by axisymmetric geometry in Figure 1. We choose z−axis through the center of the tubule, and r is chosen normal to it. The radial and axial velocities are denoted by vr (r,z) and vz (r,z), respectively.

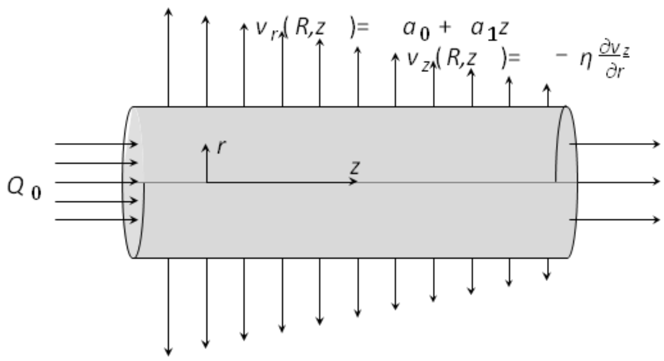

Figure 1. Geometry of the tube with linear reabsorption.

The filtrate is supplied to the proximal tubule at a constant flow rate of Q0 in the axial direction. As the fluid passes through the tubule, it becomes under the influence of linear reabsorption that varies in the axial direction. The reabsorption is assumed to be a linear function of z, and has form of a0 + a1z, where a1 < 0 and a0 > 0.

Neglecting the inertial effects, the continuity and momentum equations of the flow in cylindrical coordinate become

$$0 = \frac{1}{r}\frac{\partial}{\partial r}(r v_r) + \frac{\partial v_z}{\partial z}, \tag{1}$$

$$\frac{\partial p}{\partial r} = \mu\left[\frac{\partial^2 v_r}{\partial r^2} + \frac{1}{r}\frac{\partial v_r}{\partial r} - \frac{v_r}{r^2} + \frac{\partial^2 v_r}{\partial z^2}\right], \tag{2}$$

$$\frac{\partial p}{\partial z} = \mu \left[\frac{\partial^2 v_z}{\partial r^2} + \frac{1}{r}\frac{\partial v_z}{\partial r} + \frac{\partial^2 v_z}{\partial z^2} \right]. \tag{3}$$

where $v_r(r,z)$ and $v_z(r,z)$are radial and axial velocities, respectively; p(r,z) pressure in the tube and μ is the coefficient of viscosity. On the axis of the tubule, at r = 0,

$$v_r = 0, \qquad \frac{\partial v_z}{\partial r} = 0 \quad at\ \ r = 0. \tag{4}$$

The filtrate that becomes in contact with the tubule wall undergoes linear reabsorption and slip. The slip-length, which we denote it by η, can be interpreted as the extrapolated distance from the wall of the tubule where the axial velocity becomes zero. The axial velocity profile of such flow from the axis of the tubule to the point where vz = 0 is shown in Figure 2.

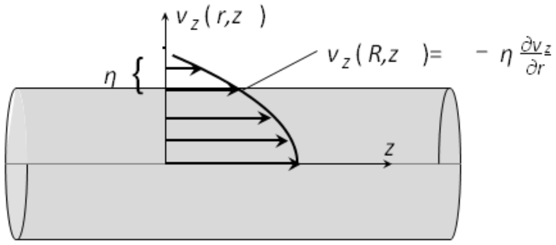

Figure 2. Slip length.

Consequently,
at r = R,

$$v_r = a_0 + a_1 z, \qquad v_z = -\eta \frac{\partial v_z}{\partial r}. \tag{5}$$

The boundary conditions at the entrance and exit of the tube are given below.

$$Q_0 = 2\pi \int_0^R r\, v_z(0,r) dr, \quad p(r,0) = p_0, \quad at\ \ z = 0 \tag{6}$$

$$p(r,L) = P_L, \qquad at\ \ z = L \tag{7}$$

Introducing vorticity $\Omega(\mathrm{r,z}) = \frac{\partial \mathrm{v_z}}{\partial \mathrm{r}} - \frac{\partial \mathrm{v_r}}{\partial \mathrm{z}}$, the system of equations in (1) can be written as

$$\frac{\partial v_r}{\partial r} + \frac{v_r}{r} + \frac{\partial v_z}{\partial z} = 0, \tag{8}$$

$$\frac{\partial p}{\partial r} = -\mu \frac{\partial \Omega}{\partial z}, \tag{9}$$

$$\frac{\partial p}{\partial z} = \mu \left\{ \frac{\partial \Omega}{\partial r} + \frac{\Omega}{r} \right\}. \tag{10}$$

Introducing stream function Ψ(r,z) such that

$$v_r = \frac{1}{r}\frac{\partial \Psi}{\partial z} \quad and \quad v_z = -\frac{1}{r}\frac{\partial \Psi}{\partial r} \tag{11}$$

equation (8) is satisfied identically by this function. Moreover, equations (9) and (10) have the following forms.

$$\frac{\partial p}{\partial r} = \frac{\mu}{r}\frac{\partial}{\partial z}(\mathbf{E}^2\Psi),$$

$$\frac{\partial p}{\partial z} = -\frac{\mu}{r}\frac{\partial}{\partial r}(\mathbf{E}^2\Psi), \tag{12}$$

where $\mathrm{E}^2 = \frac{\partial^2}{\partial \mathrm{r}^2} - \frac{1}{\mathrm{r}}\frac{\partial}{\partial \mathrm{r}} + \frac{\partial^2}{\partial \mathrm{z}^2}$.. The pressure term can be eliminated from (12) to get a single fourth order partial differential equation, which becomes the governing equation of our problem together with the boundary condition defined below.

$$E^4\Psi = 0, \tag{13}$$

where $E^{\,4} = E^{\,2}(E^{\,2})$. The boundary conditions can be described in terms of the stream function as follows.

At $r = 0$,

$$\frac{1}{r}\frac{\partial \Psi}{\partial z} = 0, \qquad \frac{\partial}{\partial r}\left(-\frac{1}{r}\frac{\partial \Psi}{\partial r}\right) = 0. \tag{14}$$

$$\frac{1}{r}\frac{\partial \Psi}{\partial z} = a_0 + a_1 z, \tag{15}$$

At $r = R$

$$A\ -\frac{1}{r}\frac{\partial \Psi}{\partial r} = -\eta\frac{\partial}{\partial r}\left(-\frac{1}{r}\frac{\partial \Psi}{\partial r}\right). \tag{16}$$

At z = 0, the flow rate at the entrance, is

$$Q_0 = 2\pi\int_0^R r\left(-\frac{1}{r}\frac{\partial \Psi(r,0)}{\partial r}\right)dr. \tag{17}$$

Boundary conditions on the pressure are

$$p = p_0,\ \text{at } z = 0\ and\ p = p_L,\ at\ z = L. \tag{18}$$

3. Solution of the problem

The homogeneous equation in (13) can be solved using separation of variables by choosing the stream function have the form of

$$\Psi(r,z) = \phi(z)F(r) + G(r), \tag{19}$$

where $\phi(z) = a_0 z + \frac{1}{2}a_1 z^2$,, and F(r) and G(r) are arbitrary functions, and a0 and a1 are the same parameters defined in the problem formulation. One can see that the choice of $\phi(z)$ is made in such a way that its derivative becomes vz(R,z), which is the reabsorption on the wall. Substitution of equation (19) in the governing equation (13) gives the following system of homogeneous equations.

$$\phi(z)\mathbf{E}^2\left(\mathbf{E}^2 F(r)\right) = 0,$$

$$2a_1\mathbf{E}^2 F(r) + \mathbf{E}^2\left(\mathbf{E}^2 G(r)\right) = 0. \tag{20}$$

The boundary conditions for the functions F(r) and G(r) are obtained with the help of equation (19) and the boundary conditions in equations (14), (15) and (17).
Boundary conditions on F(r),

$$\frac{1}{r}F(r) = 0, \quad \frac{d}{dr}\left(\frac{1}{r}F'(r)\right) = 0, \qquad at\ \ r = 0, \tag{21}$$

$$F(r) = r, \quad (\eta - r)F'(r) - r\eta F''(r) = 0, \ \ at\ \ r = R. \tag{22}$$

Boundary conditions on G(r),

$$G(r) \ = \ 0, \qquad \frac{d}{dr}\left(\frac{1}{r}G'(r)\right) = 0 \qquad at\ \ r = 0, \tag{23}$$

$$G(r) \ = \ -\frac{Q_0}{2\pi}, \quad (\eta - r)G'(r) - r\eta G''(r) = 0, \ \ at\ \ r = R. \tag{24}$$

Since F(r) and G(r) are both functions of r, equation (20) results in

$$\left[\frac{d^2}{dr^2} - \frac{1}{r}\frac{d}{dr}\right]\left[\frac{d^2}{dr^2} - \frac{1}{r}\frac{d}{dr}\right]F(r) = 0, \tag{25}$$

$$\left[\frac{d^2}{dr^2} - \frac{1}{r}\frac{d}{dr}\right]\left\{\left[\frac{d^2}{dr^2} - \frac{1}{r}\frac{d}{dr}\right]G(r) + 2a_1F(r)\right\} = 0. \tag{26}$$

At this stage, the above system of ODEs is similar to the one found in [26], but the solution turns out to be different as we enforce the slip boundary condition. In solving equation (25) we find the general solution

$$F(r) = Ar^4 + Br^2 + Cr^2\ln r + D, \tag{27}$$

where A, B, C and D are arbitrary constants. Applying the boundary conditions in equation (21) we get C = D = 0. Moreover, the boundary conditions in equation (22) gives $A = -\frac{1}{R^2(R+4\eta)}$ and $B = \frac{2R+4\eta}{R(R+4\eta)}$. Therefore, substituting these values back in equation (27) we arrive at

$$F(r) = \left[\frac{1}{R^2(R+4\eta)}\right][(2R^2+4\eta R)r^2 - r^4]. \tag{28}$$

Similarly, we integrate equation (26) to get

$$G(r) = Kr^4 + Lr^2\ln(r) + Mr^2 - \frac{2a_1}{R^2[R+4\eta]}\left\{(R^2+2\eta R)\frac{r^4}{4} - \frac{r^6}{24}\right\} + N, \tag{29}$$

where K, L, M and N are arbitrary constants, and they are obtained by applying boundary conditions in equations (23) and (24). Consequently, we get

$$L = N = 0,$$

$$K = \frac{1}{R+4\eta}\left(a_1\eta + \frac{Q_0}{2\pi R^2}\right) + \frac{a_1}{(R+4\eta)^2}\left(\eta + \frac{1}{3}R\right),$$

$$M = -\frac{Q_0}{\pi R^2}\left[\frac{R+2\eta}{R+4\eta}\right] + \frac{a_1R^2}{R+4\eta}\left[\frac{R}{12} + \frac{2\eta}{3}\right].$$

Therefore, the explicit solution to G(r),

$$\begin{aligned} G(r) \quad &= \frac{1}{R+4\eta}\left\{\frac{a_1}{12R^2}r^6 + \left[\frac{1}{R}\left(\frac{Q_0}{2\pi R^2}\right) + \frac{a_1\left(\eta + \frac{1}{3}R\right)}{R+4\eta} - \frac{a_1}{2}\right]r^4\right. \\ &\quad \left. + \left[-\frac{Q_0}{\pi R^2}(R+2\eta) + \frac{a_1R^2}{R+4\eta}\left(\frac{1}{12}R + \frac{2}{3}\eta\right)\right]r^2\right\}. \end{aligned} \tag{30}$$

Alternatively, G(r) can be written in terms of F(r) as

$$G(r) = -\frac{Q_0}{2\pi R}F(r) + \frac{a_1r^2(r^2-R^2)}{12(R+4\eta)}\left[\frac{r^2}{R^2} - \frac{R+8\eta}{R+4\eta}\right]. \tag{31}$$

The functions F(r) and G(r) described in the stream function of (19) have been found as described in equations (28) and (30). This completes the process of finding the solution to the stream function, Ψ(r,z). Using (19) together with (28) and (30) we get the explicit form of Ψ(r,z) as

$$\begin{aligned} \Psi(r,z) \quad &= \left(a_0z + \frac{a_1}{2}z^2\right)\frac{1}{R^2(R+4\eta)}[(2R^2+4\eta R)r^2 - r^4] \\ &\quad + \frac{1}{R+4\eta}\left\{\frac{a_1}{12R^2}r^6 + \left[\frac{1}{R}\left(\frac{Q_0}{2\pi R^2}\right) + \frac{a_1\left(\eta + \frac{1}{3}R\right)}{R+4\eta} - \frac{a_1}{2}\right]r^4\right. \\ &\quad \left. + \left[-\frac{Q_0}{\pi R^2}(R+2\eta) + \frac{a_1R^2}{R+4\eta}\left(\frac{1}{12}R + \frac{2}{3}\eta\right)\right]r^2\right\}. \end{aligned} \tag{32}$$

Alternatively, the stream function in (32) can be written in compact form as

$$\Psi(r,z) = -\left[\frac{Q_0}{2\pi R} - \left(a_0 z + \frac{a_1}{2}z^2\right)\right]F(r) + \frac{a_1 r^2(r^2 - R^2)}{12(R+4\eta)}\left[\frac{r^2}{R^2} - \frac{R+8\eta}{R+4\eta}\right]. \tag{33}$$

3.1. Velocity components

The radial and axial velocities are obtained using the relation in (19) and the stream function in (32). The radial component of the velocity is

$$v_r(r,z) = \frac{a_0 + a_1 z}{R+4\eta}\left[\frac{2R+4\eta}{R}r - \frac{1}{R^2}r^3\right]. \tag{34}$$

The axial component of the velocity is

$$\begin{aligned} v_z(r,z) \quad &= \frac{R}{R+4\eta}\left\{\left[1 - \left(\frac{r}{R}\right)^2\right]\left[\frac{2Q_0}{\pi R^2} - \frac{4}{R}\left(a_0 z + \frac{a_1}{2}z^2\right)\right.\right. \\ &\quad \left. - \frac{a_1 R}{2}\left(\frac{R+12\eta}{3(R+4\eta)} - \left(\frac{r}{R}\right)^2\right)\right] \\ &\quad \left. + \frac{\eta}{R}\left[\frac{4Q_0}{\pi R^2} - \frac{8}{R}\left(a_0 z + \frac{a_1}{2}z^2\right) + \frac{2a_1 R^2}{3(R+4\eta)}\right]\right\}, \end{aligned} \tag{35}$$

which can also be expressed in a compact form as

$$\begin{aligned} v_z(r,v) \quad &= \left[\frac{Q_0}{\pi R} - (2a_0 z + a_1 z^2)\right]\left[\frac{F(r)}{r^2} - \frac{r^2}{R^2(R+4\eta)}\right] \\ &\quad - \frac{a_1}{6(R+4\eta)}\left[(r^2 - R^2)\left(\frac{3r^2}{R^2} - \frac{R+12\eta}{R+4\eta}\right) - \frac{4\eta R^2}{R+4\eta}\right]. \end{aligned} \tag{36}$$

We note that in the absence of the slip parameter η the velocity components we found here are equivalent to the works reported in [1,8,26].

3.2. Extreme values of velocity components

Extreme values and the points at which they occur are obtained using basic calculus by finding the first and second order derivatives.

Extreme values of the radial velocity

Differentiating equation (34) with respect to r, we get

$$\frac{dv_r}{dr} = \frac{a_0 + a_1 z}{R+4\eta}\left[2 + \frac{4\eta}{R} - \frac{3}{R^2}r^2\right] \tag{37}$$

The critical numbers, the point where first order derivative vanishes, for (37) become

$$\frac{r}{R} = \pm\sqrt{\frac{2}{3} + \frac{4\eta}{3R}}. \tag{38}$$

Now, differentiating equation (37) and using the result in (38) we get $\frac{d^2 v_r}{dr^2} < 0$ when $\frac{r}{R} = \sqrt{\frac{2}{3} + \frac{4\eta}{3R}}$. The second order derivative test ensures that there exist extreme values for vr. The maximum radial velocity occurs at $\frac{r}{R} = \sqrt{\frac{2}{3} + \frac{4\eta}{3R}}$, and

$$v_{r_{max}} = \frac{4\sqrt{6 + \frac{12\eta}{R}}(a_0 + a_1 z)(R + 2\eta)}{9(R + 4\eta)}. \tag{39}$$

From the above results one can observe that the effect of slip parameter is significant on the maximum radial velocity and on the point where it occurs. Absence of slip condition in the above equations gives the critical number and the extreme values that are discussed in Macey [1].

Extreme values of the axial velocity

Differentiating equation (35) with respect to z, we get

$$\frac{dv_z}{dz} = \frac{R}{R + 4\eta}(a_0 + a_1 z)\left(1 + \frac{2\eta}{R} - \frac{r^2}{R^2}\right). \tag{40}$$

From the above equation $\frac{dv_z}{dz} = 0$when $z = -\frac{a_0}{a_1}$. Since z $\in$ [0,L] which is valid when $0 \leq -\frac{a_0}{a_1} \leq L$. Differentiating the same equation one more time

$$\frac{d^2 v_z}{dz^2} = -\frac{4a_1}{R + 4\eta}\left(1 + \frac{2\eta}{R} - \frac{r^2}{R^2}\right). \tag{41}$$

Extreme values of vz have the following forms.

1. Let $1 + \frac{2\eta}{R} - \frac{r^2}{R^2} < 0$, which is the same as $\frac{r^2}{R^2} > 1 + \frac{2\eta}{R}$

a. When $a_1 > 0$, then $\frac{d^2 v_z}{dz^2} > 0$. Thus, v_z has minimum at $z = -\frac{a_0}{a_1}$.

b. When $a_1 < 0$, then $\frac{d^2 v_z}{dz^2} < 0$. Thus, v_z has maximum at $z = -\frac{a_0}{a_1}$.

2. Let $1 + \frac{2\eta}{R} - \frac{r^2}{R^2} > 0$, which is the same as $\frac{r^2}{R^2} < 1 + \frac{2\eta}{R}$

a. When $a_1 > 0$, then $\frac{d^2 v_z}{dz^2} < 0$. Thus Thus v_z has maximum at $z = -\frac{a_0}{a_1}$.

b. When $a_1 < 0$, then $\frac{d^2 v_z}{dz^2} > 0$. Thus v_z has minimum at $z = -\frac{a_0}{a_1}$.

For various scenario, the axial velocity attains its extreme values at $z = -\frac{a_0}{a_1}$. Specifically, for a decreasing linear reabsorption, $a_1 < 0$, the axial velocity attains its minimum value inside the tubule when $z = -\frac{a_0}{a_1}$. If one removes the slip coefficient η, the extreme values of the axial and radial velocities found above become equivalent with their counterpart that was found in [8].

3.3. Pressure distribution

Pressure has an important effect both in glomerular filtration as well as proximal tubule reabsorption process. This pressure is analytically solved from equation (12) and the stream function by substituting velocity components (34) and (35) in equation (9) and (10) we get

$$\frac{\partial p}{\partial z}=\frac{\mu}{R+4\eta}\left[-\frac{8Q_0}{\pi R^3}+\frac{16(a_0 z+\frac{a_1}{3}z^2)}{R^2}+2a_1\left(\frac{R+12\eta}{3(R+4\eta)}-\frac{R+4\eta}{R}-\frac{2r^2}{R^2}\right)\right],$$

$$\frac{\partial p}{\partial r}=-\frac{8\mu r(a_0+a_1 z)}{R^2(R+4\eta)}. \tag{42}$$

By integrating the above two equations, the following expression to the pressure difference is obtained.

$$\begin{aligned} p(r,z)-p(0,0) \quad &=\frac{\mu}{R^2(R+4\eta)}[\frac{-8Q_0 z}{\pi R}-4a_0 r^2+8(a_0 z^2+\frac{a_1}{3}z^3) \\ &+2a_1 R^2 z\left(\frac{R+12\eta}{3(R+4\eta)}-\frac{R+4\eta}{R}-\frac{2r^2}{R^2}\right)]. \end{aligned} \tag{43}$$

When η = 0, the above equation agrees with the pressure difference given in the work of Macey in [1].

3.3.1. The mean pressure distribution

The average pressure distribution is defined as

$$\bar{p}(z)=\frac{2}{R^2}\int_0^R r\,[p(r,z)-p(0,0)]dr. \tag{44}$$

Using equation (43), the average pressure is obtained as

$$\begin{aligned} \bar{p}(z) \quad &=\frac{\mu}{R^2(R+4\eta)}\left\{-\frac{8Q_0 z}{\pi R}-2a_0 R^2+8(a_0 z^2+\frac{a_1}{3}z^3)\right. \\ &\left.-2a_1 R^2 z\left(\frac{2R}{3R+12\eta}+\frac{R+4\eta}{R}\right)\right\}. \end{aligned} \tag{45}$$

3.3.2. The mean pressure drop

The mean pressure drop between the entrance, $z=0$, and exit, $z=L$, of a proximal tubule is expressed as $\Delta\bar{p}(L)=\bar{p}(0)-\bar{p}(L)$. This pressure drop is obtained from equation (45). This pressure drop is expressed as

$$\Delta\bar{p}(L)=\frac{\mu L}{R^2(R+4\eta)}\left\{\frac{8Q_0}{\pi R}-8L\left(a_0+\frac{a_1}{3}L\right)+2a_1 R^2\left(\frac{2R}{3(R+4\eta)}+\frac{R+4\eta}{R}\right)\right\}. \tag{46}$$

The average pressure drop obtained by Macey [1] and Achala [8] can be obtained from the above equation when η = 0, i.e with the absence of slip condition.

3.4. Fractional reabsorption

The axial flow rate inside a tube is obtained from the following relation

$$Q(z) = 2\pi \int_0^R r\, v_z dr = 2\pi \int_0^R r\, (-r \frac{\partial \Psi}{\partial r}) dr$$

The above integral gives the flow rate at a point z as

$$Q(z) = -2\pi(\Psi(R,z) - \Psi(0,z)) \quad (47)$$

The fractional reabsorption is the amount of original filtrate that has been reabsorbed through the tubule wall. If α represents the fraction of original fluid that has been reabsorbed when the fluid reaches the exit, at z = L, then

$$\alpha = \frac{Q_0 - Q_L}{Q_0} \qquad or \qquad Q_L = (1-\alpha)Q_0. \quad (48)$$

The axial flow rate at the exit of tubule, QL, is computed from equation (48) and (33).

$$Q_L = Q_0 - 2\pi R \left(a_0 L + \frac{a_1}{2} L^2\right). \quad (49)$$

The above equation shows that the axial flow rate is independent of the slip parameter η. Inserting equation (48) in the above equation, we get

$$Q_L = Q_0 - 2\pi R \left(a_0 L + \frac{a_1}{2} L^2\right). \quad (50)$$

If $\mathrm{a}_1 = 0$ in the above equation, this result matches with the one obtained by Macey . If the reabsorption starts at the entrance of the tubule, then the rate, a_1, of linear reabsorption, $\mathrm{a}_0 + \mathrm{a}_1 \mathrm{z}$, has a minimum value of $-\frac{2\mathrm{a}_0}{\mathrm{L}}$.

$$a_1 \geq -\frac{2a_0}{L}. \quad (51)$$

The mean pressure drop in the tubule can be expressed in terms of the average flow rate between the entrance and exist.

$$\Delta\bar{p}(L) \quad = \frac{\mu L}{R^2(R+4\eta)} \left\{ \frac{8}{\pi R} \left(\frac{Q_L + Q_0}{2} \right) + a_1 \left(\frac{4R^3}{3R+12\eta} + 2R(R+4\eta) + \frac{4L^2}{3} \right) \right\}. \quad (52)$$

Moreover, the mean pressure drop have the following upper and lower limits.

$$\frac{\mu L}{R^2(R+4\eta)}\left\{\frac{4Q_0}{\pi R}+a_1\left(\frac{4R^3}{3R+12\eta}+2R(R+4\eta)+\frac{4L^2}{3}\right)\right\}\leq \Delta\bar{p}(L)\leq$$
$$\frac{\mu L}{R^2(R+4\eta)}\left\{\frac{8Q_0}{\pi R}+a_1\left(\frac{4R^3}{3R+12\eta}+2R(R+4\eta)+\frac{4L^2}{3}\right)\right\}.$$

The above relation agrees with the work done by Macey [1] when a1 and η are set to be zero.

3.5. Wall shear stress

Shear stress is defined as

$$\tau_w|_{r=R}=-\mu\left(\frac{\partial v_z}{\partial r}+\frac{\partial v_r}{\partial z}\right)_{r=R}. \tag{53}$$

Differentiating equations (34) and (35) according to the above relation, we get the shear stress as

$$\tau_w|_{r=R}=\frac{-\mu}{R+4\eta}\left\{-\frac{4Q_0}{\pi R^2}+\frac{8}{R}\left(a_0z+\frac{a_1}{2}z^2\right)+a_1\left(R+4\eta-\frac{2R^2}{3R+12\eta}\right)\right\}. \tag{54}$$

3.6. Some special cases

Special cases of the solution to the stream function, axial and radial velocities are discussed and compared to results obtained by other researchers.

Case 1: Slip flow with constant reabsorption

In this case parameters $a_1=0$ and $\eta\neq 0$, thus equations, thus equations (32), (34) and (35) become

$$\psi(r,z)=-\left(\frac{Q_0}{2\pi R}-a_0z\right)F(r),$$

$$v_r(r,z)=a_0\frac{F(r)}{r},$$

$$v_z(r,z)=\left(\frac{Q_0}{\pi R}-(2a_0z+a_1z^2)\right)\left(\frac{F(r)}{r^2}-\frac{r^2}{R^2(R+4\eta)}\right),$$

$$\bar{p}(z)=\frac{\mu}{R^2(R+4\eta)}\left[-\frac{8Q_0z}{\pi R}-2a_0(R^2-4z^2)\right],$$

$$\tau_w|_{r=R}=\frac{-\mu}{R+4\eta}\left\{-\frac{4Q_0}{\pi R^2}+\frac{8a_0z}{R}\right\}. \tag{55}$$

Case 2: No-slip flow with linear reabsorption

In this case parameters η = 0 and a1 6= 0, thus equations (32), (34) and (35) become

$$\psi(r,z) \;= -\left[\frac{Q_0}{2\pi R} - (a_0 z + \frac{a_1}{2} z^2)\right] F(r) + \frac{a_1 r^2 (r^2 - R^2)^2}{12R^3},$$

$$v_r(r,z) \;= (a_0 + a_1 z)\left(\frac{2r}{R} - \frac{r^3}{R^3}\right),$$

$$v_z(r,z) \;= \left[\frac{Q_0}{\pi R} - (2a_0 z + a_1 z^2)\right]\left[\frac{F(r)}{r^2} - \frac{r^2}{R^3}\right] - \frac{a_1}{6R^3}(r^2 - R^2)(3r^2 - R^2),$$

$$\bar{p}(z) \;= \frac{\mu}{R^3}\left[-\frac{8Q_0 z}{\pi R} - 2a_0(R^2 - 4z^2) + \frac{2a_1}{3}(4z^3 - 5R^2 z)\right],$$

$$\tau_w|_{r=R} \;= \frac{-\mu}{R + 4\eta}\left\{-\frac{4Q_0}{\pi R^2} + \frac{8}{R}\left(a_0 z + \frac{a_1}{2} z^2\right) + \frac{a_1 R}{3}\right\}. \tag{56}$$

This axial velocity matches with the result reported by Macey [1] and Achala [8].

Case 3: No-slip flow with constant reabsorption

In this case parameters η = 0 and a1 = 0. This is a special case of case 2, where a1 = 0. The three

$$\psi(r,z) \;= -\left[\frac{Q_0}{2\pi R} - (a_0 z + \frac{a_1}{2} z^2)\right] F(r),$$

$$v_r(r,z) \;= a_0\left(\frac{2r}{R} - \frac{r^3}{R^3}\right),$$

$$v_z(r,z) \;= \left[\frac{Q_0}{\pi R} - (2a_0 z + a_1 z^2)\right]\left[\frac{F(r)}{r^2} - \frac{r^2}{R^3}\right],$$

equations under case 2 become

$$\bar{p}(z) \;= \frac{\mu}{R^3}\left[-\frac{4Q_0}{\pi R^2} + \frac{8a_0 z}{R}\right],$$

$$\tau_w|_{r=R} \;= \frac{-\mu}{R}\left\{-\frac{4Q_0}{\pi R^2} + \frac{8a_0 z}{R}\right\}. \tag{57}$$

4. Results and discussion

All physical quantities discussed in the previous sections are made to be dimensionless, so that the new, but equivalent non-dimensional parameters, are used in computations and graphing.

$$z^* = \frac{z}{L},\ r^* = \frac{r}{R},\ v_r^* = \frac{v_r}{a_0},\ v_z^* = \frac{v_z}{a_0},\ p^* = \frac{p}{\frac{a_0\mu}{R}},\ Q_0^* = \frac{Q_0}{a_0 R^2},$$

$$Q^* = \frac{Q}{a_0 R^2},\ \eta^* = \frac{\eta}{R},\ \tau^* = \frac{\tau}{\frac{\mu a_0}{R}},\ \Psi^* = \frac{\Psi}{a_0 R^2},\ a_1^* = \frac{a_1}{\frac{a_0}{R}}.$$

In previous sections we have found physiological quantities velocity components, pressure distribution, fractional reabsorption and shear stress of the flow. In order to evaluate performance of our result, we consider proximal tubule of rat kidney using the data given in [1,8,9] by:

$$\mu = 7 \times 10^{-3}\, dyn.sec/cm^2,\ Q_0 = 4 \times 10^{-7}\, cm^3/sec,$$

$$R = 10^{-3}\, cm \text{ and } L = 1\, cm.$$

According to Curthoys et al. [27] the proximal tubule is a part of the renal tubule next to the glomerulus, contributes for fluid, electrolyte, and nutrient homeostasis by reabsorbing 60–70% of water and sodium chloride. The remaining part of the filtrate pass through the tubule to be excreted in the form of urine.

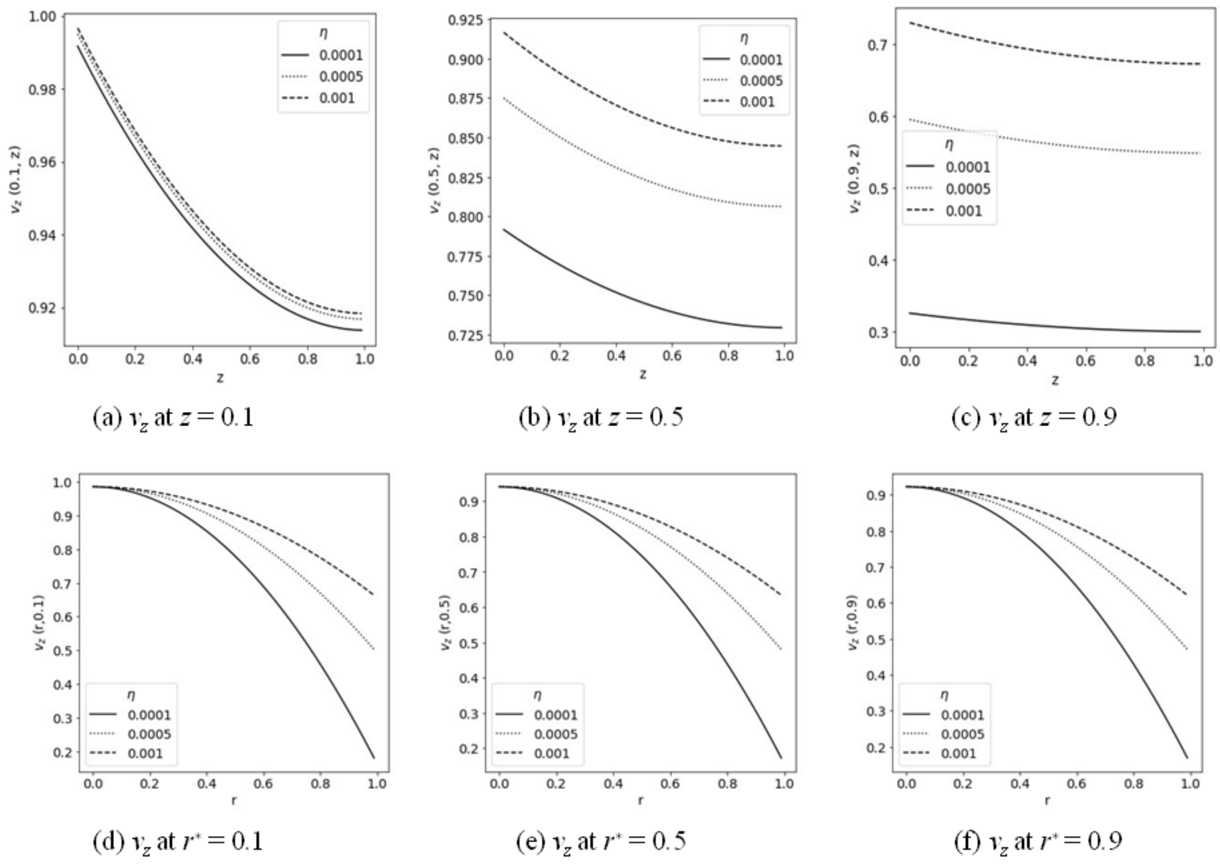

Figure 3. Effect of η on axial velocity.

Under normal condition the fractional filtrate that has been absorbed in the proximal tubule would approximately be $\alpha = 0.8$. The simpler case of constant reabsorption, (51) gives $a_0 = \frac{\alpha Q_0}{2*\pi R L}$. Moreover, equation (52) is used to estimate the lower limit of a1. In the problem formulation, we have defined the linear reabsorption as a0 + a1z, and it is assumed to be a decreasing function with a1 < 0. Since the velocity components, average pressure drop and the wall shear stress are all depend on the linear reabsorption rate, it is understood that the parameter a1 affects their profile.

The radial velocity component is observed to be very sensitive to changes in a1 that results in back flow either in radial or axial direction.

In Figure 3, the effect on axial velocity is shown at various locations in the tubule. This axial velocity is observed to increase with η increases at every location we have selected for analysis. We also observe that the effect from η on vz is minimal near the axis and the entrance of the tubule. This effect gradually grows as we go further from the axis to the wall and from the entrance to the exit of the tubule. Moreover, vz is higher for a well lubricated proximal tubule than the tubule that is not lubricated. This is because the smoothness of the wall gives rise to a non-vanishing axial velocity near the wall, and hence results in a longer slip-length.

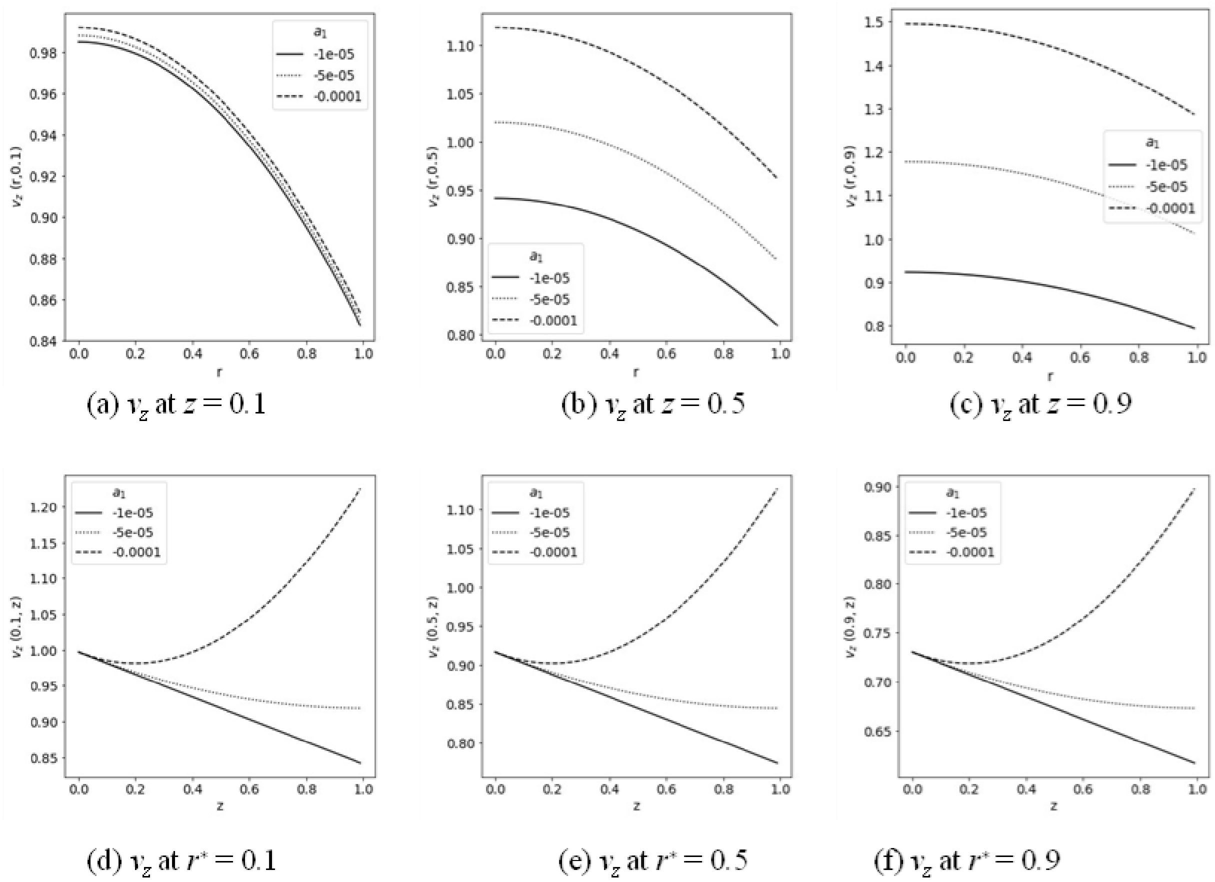

(a) v_z at $z = 0.1$ (b) v_z at $z = 0.5$ (c) v_z at $z = 0.9$

(d) v_z at $r^* = 0.1$ (e) v_z at $r^* = 0.5$ (f) v_z at $r^* = 0.9$

Figure 4. Effect of a_1 on axial velocity.

Figure 4 indicates that there is a strong relationship between a1 and the axial velocity at various locations in the tubule. Both along the radial and axial directions, vz increases as |a1| increases. This is interpreted as smaller reabsorption gives rise to greater axial velocity. Near the mouth of the tubule, Figure 4d–4f, the change in a1 is not that significant, but as we go further along the tubule this goes up so that the effect becomes very high at the exit. Furthermore, the effect of a1 is very small near the axis of the tubule, and as we go further to the wall this effect becomes very significant.

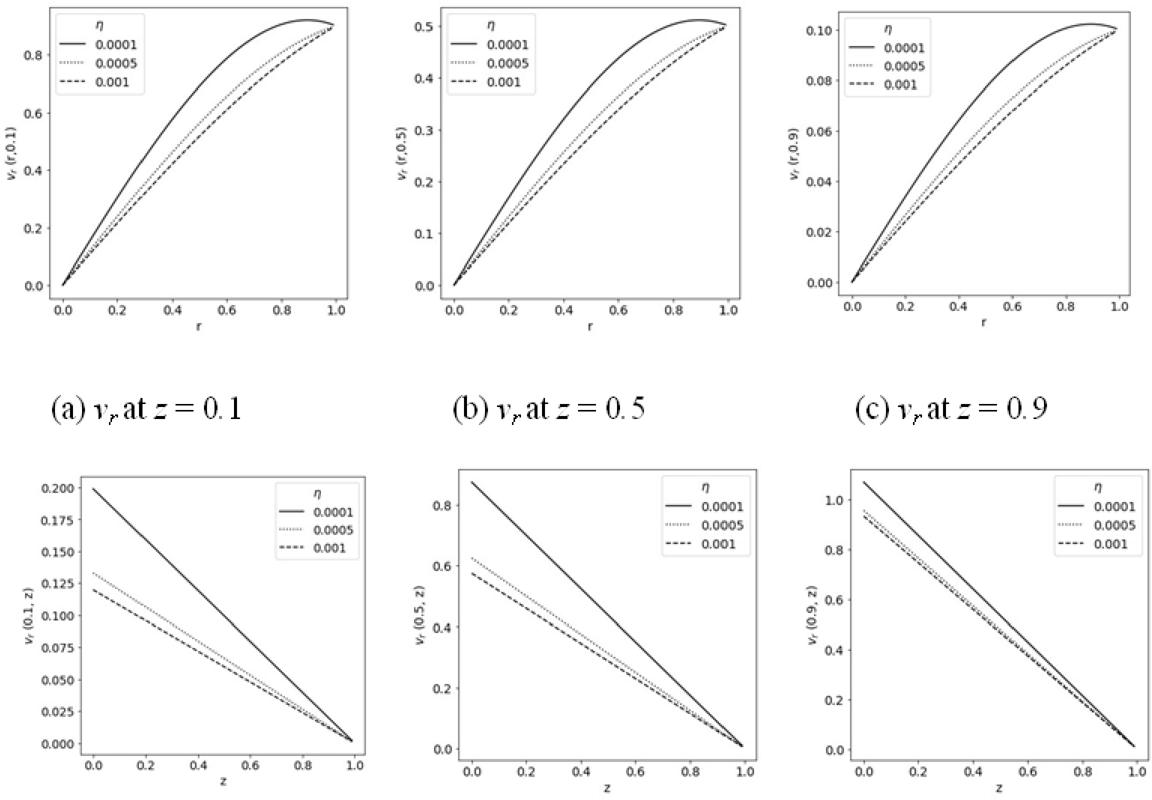

(a) v_r at $z = 0.1$ (b) v_r at $z = 0.5$ (c) v_r at $z = 0.9$

(d) v_r at $r^* = 0.1$ (e) v_r at $r^* = 0.5$ (f) v_r at $r^* = 0.9$

Figure 5. Effect of η on radial velocity.

When the slip-length is extended, the radial velocity is observed to decrease as shown in Figure 5. Near the axis and close to the wall of the tubule, the effect of η on vr is not significant. On the other hand, at the entrance the effect of η is very significant, and this effect diminishes as we go along the tubule.

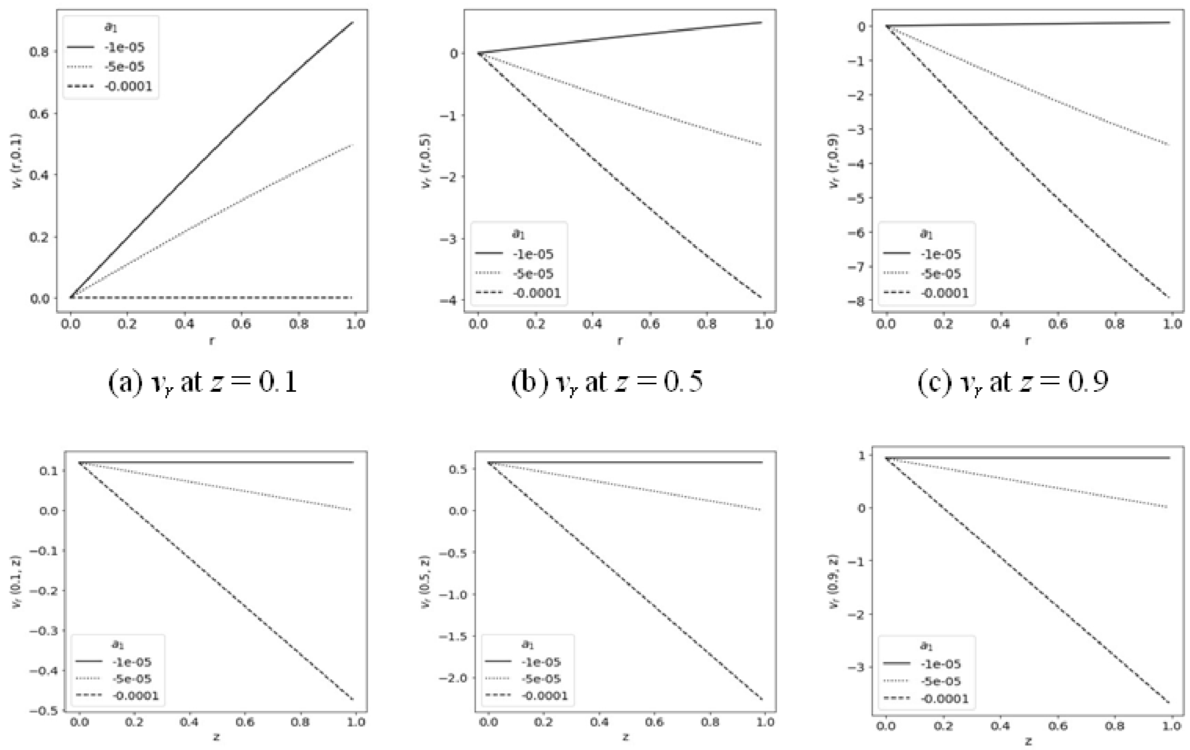

(a) v_r at $z = 0.1$ (b) v_r at $z = 0.5$ (c) v_r at $z = 0.9$

(d) v_r at $r^* = 0.1$ (e) v_r at $r^* = 0.5$ (f) v_r at $r^* = 0.9$

Figure 6. Effect of a_1 on radial velocity.

In Figure 6 we choose $a_1 = -10^{-5}, -5 \times 10^{-5}$ and 10^{-4} to observe how vr changes at various locations in the tubule. Except when a1 = -10^{-5}, the radial velocity is negative for most of the locations chosen. This negative velocity indicates the back flow both in the axial and radial directions. The reason for back flow is that when |a1| gets bigger, the reabsorption, a0+a1z, becomes smaller and goes to negative which gives rise to accumulation of filtrate in the tubule. The reabsorption vanishes at $z = -\frac{a_0}{a_1}$, beyond this point the inward flow starts to develop in the radial direction. For example, if $z = -\frac{a_0}{-10 * a_0} = 0.1$, the reabsorption will stop early at a point $z = 0.1$, and from this point on ward the filtrate will flow back into the tubule. In Figures 6d–6f, one can see that the back flow is initiated from the end of the tubule towards it mouth. This is because, as shown in Figure 6c magnitude of radial velocity is greater at z = 0.9, which results in higher accumulation of filtrates that have flown back in radial direction.

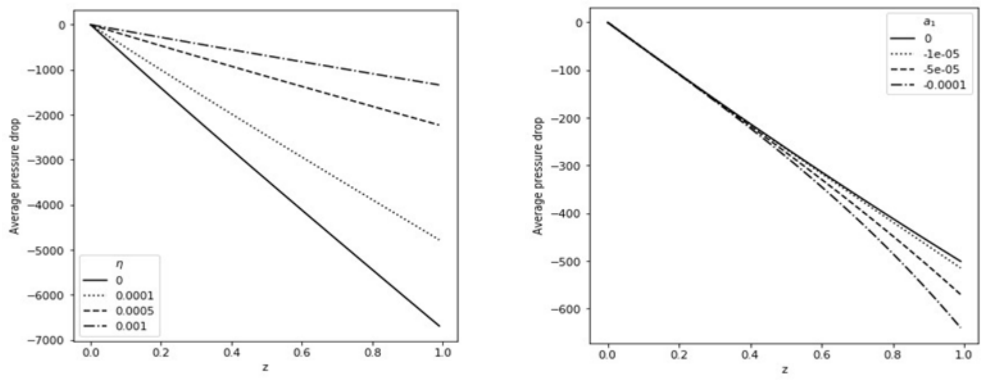

(a) Average pressure drop for values of η (b) Average pressure drop for values of a_1

Figure 7. Average pressure drop at *z*.

As plotted in Figure 7a the average pressure drop decreases with η increases at every point in the tubule. This is because, as η is further away from the wall it increases the axial velocity near the wall, which in turn reduces the pressure drop. The pressure drop between the entrance and exit of the tubule also shows similar dependence on η. In Figure 7b, the average pressure drop increases with |a1|. Even though, the effect of a1 is not much significant on the average pressure drop at the beginning, but it gradually grows as we go to the exit.

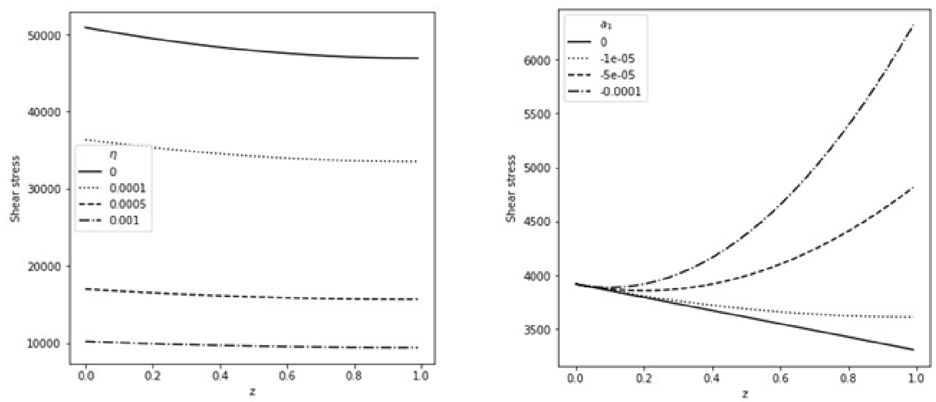

(a) Wall shear stress for η (b) Wall shear stress for a_1

Figure 8. Wall shear stress at *z*.

In addition to these, the wall shear stress is also influenced by the change in η. Figure 8a shows that the higher slip-length gives the lowers shear stress on the wall. When η = 0.001, which is ten times the radius of the tubule, the shear stress is nearly constant. Another physiological quantity that is affected by changing a1 is the wall shear stress. As shown in Figure 8b it is inversely related with |a1|. Specifically, near the end of the tubule the effect is very significant.

From Table 1, it is noted that the decreasing value of reabsorption velocity causes to reduce the fractional reabsorption but the mean pressure drop in the lubricated proximal tubule increases with the decreasing value of reabsorption velocity. The increasing values of slip parameter show that pressure rise decreases and decrease in pressure rise is high when fractional reabsorption is 90%. Table 2 indicate that Δp is inversely proportional to reabsorption velocity, fractional reabsorption and slip parameter. It is noted through Table 3 and Table 4 that pressure difference increases with the decreasing values of linear reabsorption velocity and fractional reabsorption but decreases with the increasing values of slip parameter.

Table 1. Fractional reabsorption, pressure difference and reabsorption velocity of fluid for slip flow with constant reabsorption (a1 = 0, η ≠0).

η	α	a_0 *cm/*sec	$\overline{\Delta p}(0.21)$ *dyn/cm*^{2}
0.2			15994.5
0.4			7999.74
0.6	90%	1.08	5333.71
0.8			4000.49
1.0			3200.49
0.2			17454.2
0.4			8729.8
0.6	80%	0.96	5820.48
0.8			4365.58
1.0			3492.58
0.2			18913.8
0.4			9459.87
0.6	70%	0.84	6307.24
0.8			4730.68
1.0			3784.66
0.2			21954.8
0.4			10980.8
0.6	50%	0.59	7321.33
0.8			5491.28
1.0			4393.16

It is noted through Table 3 and Table 4 that pressure difference increases with the decreasing values of linear reabsorption velocity and fractional reabsorption but decreases with the increasing values of slip parameter. It is observed that pressure difference increases with the decreasing values of fractional reabsorption, uniform reabsorption and linear reabsorption velocity. The analysis shows that urine flow through lubricated proximal tubule requires the less amount of pressure difference when the lubrication on the wall and fractional reabsorption on the wall is high whereas the pressure difference is high for the linear reabsorption as compared to the uniform reabsorption.

Table 2. Fractional reabsorption, pressure difference and reabsorption velocity of fluid for slip flow with linear reabsorption. (a1 ≠ 0, η ≠ 0).

η	α	a_0 *cm/*sec	a_1 *cm/*sec	$\overline{\Delta p}(0.21)$ *dyn/cm*^{2}
0.2				24696.6
0.4				12322.3
0.6	90%	1.08	−10.29	8195.86
0.8				6132.31
1.0				4894.08
0.2				25183.7
0.4				12569.3
0.6	80%	0.96	−9.14	8362.76
0.8				6259.15
1.0				4996.88
0.2				25679.3
0.4				12820.5
0.6	70%	0.84	−8	8532.43
0.8				6388.06
1.0				5101.34
0.2				26699.1
0.4				13337.5
0.6	50%	0.59	−5.61	8881.74
0.8				6653.53
1.0				5316.48

Table 3. Fractional reabsorption, pressure difference and reabsorption velocity of fluid for no slip flow with linear reabsorption (a1 ≠ 0, η = 0).

α	a_0 *cm/*sec	a_1 *cm/*sec	$\overline{\Delta p}(0.21)$ *dyn/cm*^{2}
90%	1.08	−10.29	3.96346×10^7
80%	0.96	−9.14	4.04038×10^7
70%	0.84	−8	4.11867×10^7
50%	0.59	−5.61	4.27973×10^7

Table 4. Fractional reabsorption, pressure difference and reabsorption velocity of fluid for no slip flow with constant reabsorption (a1 = 0, η = 0).

α	90%	80%	70%	50%
a_0 *cm/*sec	1.08	0.96	0.84	0.59
$\overline{\Delta p}(.21)$ *dyn/cm*^{2}	2.56072×10^7	2.79441×10^7	3.02811×10^7	3.51497×10^7

4.1. Application to the lubricated proximal renal tubule

We have used physiological data of human kidneys to get the values of reabsorption velocity and average pressure difference (Δp). Since length of proximal renal tubule in human body varies from 0.12 cm−0.21 cm. Therefore, we have chosen L = 0.21 cm. Radius of proximal renal tubule in human body varies between 0.00025 cm−0.0005 cm, therefore radius of proximal renal tubule is considered as R = 0.0005 cm. The present model suggests that the viscosity of urine in proximal renal tubule is $\mu = 6.9 \times 10^{-3}$ dynsec/cm^2 and flow rate of urine is $Q_0 = 7.9 \times 10^{-4}$ cm^3/sec. In Table (1–4) we have calculated reabsorption velocity and mean pressure drop (Δp) with the help of mathematical expression given in Eq. 52 and Eq. 53. In normal circumstances glomerulus pressure is believed to be about 45 mmHg which is a higher pressure than that found in capillaries elsewhere in the body.

5. Conclusion

In this paper, we obtain exact solution for two-dimensional flow through a proximal tubule with linear reabsorption and slip in cylindrical coordinate. The coupled partial differential equations are converted into a single equation in terms of the stream function. The exact expressions for velocity components, pressure distribution, average pressure drop, the wall shear stress, and fractional reabsorption are explicitly obtained.

It is found that extreme values for the radial velocity exist at r =$r = R\sqrt{\frac{2}{3} + \frac{4\eta}{3R}}$; for the axial velocity, the same occur at $z = -\frac{a_0}{a_1}$. For the fractional reabsorption α, it is also found that $a_0 + \frac{a_1 L}{2} = \frac{\alpha Q_0}{2\pi RL}$. In addition to this, for a reabsorption to occur $a_1 \geq -\frac{2a_0}{L}$, otherwise back flow would occur in the radial direction. Furthermore, from this work the following are also be observed.

The physiological quantities discussed above depends on the slip-length and the reabsorption rate. There is direct relationship between the axial velocity and η, which is minimum at the beginning, but it gradually grows along the tubule. On the other hand, the radial velocity component decreases when η is increased. The average pressure drop and shear stress decrease as η is reduced.

The axial velocity increases with increase in the value of |a1|. This relationship is interpreted as a smaller reabsorption gives rise to greater axial velocity. It is found that the radial velocity to be very sensitive to changes in the reabsorption rate, a1. When the value of $-\frac{a_0}{a_1}$ is very small, the reabsorption stops at early stage and it is followed by a back flow. The average pressure drop increases with |a1|, which gradually grows from the entrance to exit of the proximal tubule. The wall shear stress is inversely related with |a1|, and this relationship is very significant as one goes to the exit.

The mathematical formulations and the analysis in this work are theoretical; assumptions were taken when the exact solutions are obtained. The smoothness or lubrication of the proximal tubule contributes to change in the slip-length η. Moreover, the gradient of absorption rate affects the velocity. We would like to mention that experimental work needs to be done to fully understand the flow nature and parameters that influence physiological quantities. This experiment includes the effect of reabsorption gradient a1 and η on velocity, pressure, flow rate and the shear stress.

Acknowledgment

Getinet Gawo would like to thank Pennsylvania State University, York Campus for the financial support provided for this work through York Campus Advisory Board Scholarly Activity Grant.

Conflict of interest

All authors have no conflict of interest.

Authors contribution

A.M Siddiqui provided the formulation of the problem, defining governing equations and boundary conditions and supervised whole paper. G. Gawo solved the governing equations and results are compared with previous works, and results are also implemented on rat kidney data. K.Maqbool revised the literature review, implemented the result on human kidney and draft the result and handled the paper submission process.

References

1. Macey RI (1963) Pressure flow patterns in a cylinder with reabsorbing walls. *B Math Biophys* 25: 1–9.
2. Berman AS (1953) Laminar flow in channels with porous walls. *J Appl Phys* 24: 1232–1235.
3. Yuan SW (1955) Laminar pipe flow with injection and suction through a porous wall. *Princeton Univ nj James Forrestal Research Center* 78: 719–724.
4. Yuan SW (1956) Further investigation of laminar flow in channels with porous walls. *J Appl Phys* 27: 267–269.
5. Terrill RM (1982) An exact solution for flow in a porous pipe. *Z Angew Math Phys* 33: 547–552.
6. Macey RI (1965) Hydrodynamics in the renal tubule. *B Math Biophys* 27: 117.
7. Gilmer GG, Deshpande VG, Chou CL, et al. (2018) Flow resistance along the rat renal tubule. *Am J Physiol-Renal* 315: F1398–F1405.
8. Achala LN, Shreenivas KR (2011) Two dimensional flow in renal tubules with linear model. *Adv Appl Math Biosci* 2: 47–59.
9. Siddiqui AM, Haroon T, Shahzad A (2016) Hydrodynamics of viscous fluid through porous slit with linear absorption. *Appl Math Mech* 37: 361–378.
10. Navier C (1823) Thesis on the Laws of Motion of Fluids. *Memoirs of the Royal Academy of Sciences of the Institut de Franc*e 6: 389–440.
11. Darrigol O (2002) Between hydrodynamics and elasticity theory: the first five births of the Navier-Stokes equation. *Arch Hist Exact Sci* 56: 95–150.
12. Mooney M (1931) Explicit formulas for slip and fluidity. *J Rheol* (1929–1932) 2: 210–222.
13. Chauffoureaux JC, Dehennau C, Van Rijckevorsel J (1979) Flow and thermal stability of rigid PVC. *J Rheol* 23: 1–24.
14. Lau HC, Schowalter WR (1986) A model for adhesive failure of viscoelastic fluids during flow. *J Rheol* 30: 193–206.
15. Cohen Y, Metzner AB (1985) Apparent slip flow of polymer solutions. *J Rheol* 29: 67–102.
16. Hatzikiriakos SG, Dealy JM (1991) Wall slip of molten high density polyethylene. I. Sliding plate rheometer studies. *J Rheol* 35: 497–523.
17. Hatzikiriakos SG, Dealy JM (1992) Wall slip of molten high density polyethylenes. II. Capillary rheometer studies. *J Rheol* 36: 703–741.
18. Rao IJ, Rajagopal KR (1999) The effect of the slip boundary condition on the flow of fluids in a channel. *Acta Mech* 135: 113–126.

19. Elshahed M (2004) Blood flow in capillary under starling hypothesis. *Appl Math Comput* 149: 431–439.
20. Singh R, Laurence RL (1979) Influence of slip velocity at a membrane surface on ultrafiltration performance—I. Channel flow system. *Int J Heat Mass Tran* 22: 721–729.
21. Chu ZKH (2000) Slip flow in an annulus with corrugated walls. *J Phys D: Appl Phys* 33: 627.
22. Beavers GS, Joseph DD (1967) Boundary conditions at a naturally permeable wall. *J Fluid Mech* 30: 197–207.
23. Priezjev NV, Darhuber AA, Troian SM (2005) Slip behavior in liquid films on surfaces of patterned wettability: Comparison between continuum and molecular dynamics simulations. *Phys Rev E* 71: 041608.
24. Palatt PJ, Sackin H, Tanner RI (1974) A hydrodynamic model of a permeable tubule. *J Theor Biol* 44: 287–303.
25. Siddiqui AM, Haroon T, Kahshan M, et al. (2015) Slip effects on the flow of Newtonian fluid in renal tubule. *J Comput Theor Nanos* 12: 4319–4328.
26. Kapur JN (1988) *Mathematical Modelling*. New Age International.
27. Curthoys NP, Moe OW (2014) Proximal tubule function and response to acidosis. *Clin J Am Soc Nephro* 9: 1627–1638.